2020

Generation of Large-Volume High-Pressure Plasma by Spatiotemporal Control of Space Charge

Shirshak K. Dhali
Old Dominion University

Original Publication Citation

Dhali, S. K. (2020). Generation of large-volume high-pressure plasma by spatiotemporal control of space charge. *AIP Advances, 10*(3), 035002. doi:10.1063/1.5143923

Generation of large-volume high-pressure plasma by spatiotemporal control of space charge

Cite as: AIP Advances **10**, 035002 (2020); https://doi.org/10.1063/1.5143923
Submitted: 30 December 2019 . Accepted: 08 February 2020 . Published Online: 02 March 2020

Shirshak K. Dhali

Generation of large-volume high-pressure plasma by spatiotemporal control of space charge

Cite as: AIP Advances 10, 035002 (2020); doi: 10.1063/1.5143923
Submitted: 30 December 2019 • Accepted: 8 February 2020 •
Published Online: 2 March 2020

Shirshak K. Dhali[a)]

AFFILIATIONS

Department of Electrical and Computer Engineering, Old Dominion University, Norfolk, Virginia 23529, USA

[a)]Author to whom correspondence should be addressed: sdhali@odu.edu

ABSTRACT

Any attempt to scale pressure and volume of nonthermal plasma usually leads to instabilities due to the formation of localized space charge. The control of the plasma is limited by the discharge geometry, type of excitation, and gas composition. This article explores the possibility of controlling the space charge in a discharge with a spatially and temporally varying electric field. It is shown that a phase-staggered sinusoidal excitation to a set of conformal azimuthal electrodes in a cylindrical geometry leads to a traveling electric field. Simulations show that in space charge dominated transport, the charged species are dispersed both in the radial and azimuthal directions. This will lead to better control of the space charge and stable discharges near atmospheric pressures.

There was a concerted effort to advance the understanding of non-equilibrium air plasma at atmospheric pressure through a multi-university research initiative (MURI) entitled "Air Plasma Ramparts."[1] The progress in this area has only been incremental since then. Achieving a large-volume glow-like discharge at atmospheric pressure has been challenging.[2,3] A search of commercially available state-of-the-art glow-like atmospheric plasma devices for industrial applications quickly reveals their limitations: they are either narrow tubular devices or wide slits with narrow openings. Some of these sources are finding application in the emerging field of plasma medicine, but the requirements are very different for an industrial plasma. Often to overcome the size limitation, multiple sources are put together in various configurations to process larger surfaces. Most of the improvements proposed have been incremental.

By its very nature, the generation of large-volume plasmas under ambient conditions is limited by instabilities arising due to the space charge dominated transition from Townsend discharge to filamentary streamer discharges when an attempt is made to scale up. For a glow discharge operating at the normal region of the voltage–current characteristic, the current density scales with square of the pressure.[4,5] Therefore, as the pressure is increased, the cross section of the discharge is reduced for a constant discharge current, leading to a small discharge volume and high power densities, which leads to instabilities. Paschen's minimum pressure times gap distance (pd) for typical gases is about 0.5 Torr cm.[6,7] At atmospheric pressure (760 Torr), the minimum breakdown voltage would occur at very small gap distances of the order of μm. In most practical applications, the discharge operates in the linear region of the right-hand side of the Paschen curve. This requires several kV to initiate a discharge in typical gases with a few mm gap. This is clearly one of the difficulties in scaling. In addition, the energy pumped into a plasma primarily goes into gas heating, which is very inefficient. The mean electron energy determines the pathways leading to reactions and partitioning of the energy into desired species production and not to gas heating. The electron kinetics primarily depends on the gas composition and the local electric field. Some of this can be controlled by tailoring the gas composition, which involves the expensive heavy use of He as the carrier gas.[8,9]

For a given operating gas composition, the characteristics of a plasma can be primarily controlled by the electrode geometry and the power source, which can be DC, AC, or pulsed. Traditional methods of exciting electrodes are spatially fixed and temporarily varying.[8] As a result, the space charge at atmospheric pressure tends to be spatially confined, resulting in non-uniformity and localized electric field enhancement, which eventually leads to instability as the discharge gap distance is increased.

When a sinusoidal alternating field is applied to a neutral gas, the processes leading to the electrical breakdown are different from those under steady fields, depending on the frequency of the alternating field. At low frequencies, the change in the field is slow compared to discharge formation time, which is in the sub-microsecond to nanosecond time scale. At these frequencies, the discharge shows the characteristics similar to the DC breakdown determined by the static breakdown voltage. Above a critical frequency, the change in the polarity of the electrode is fast enough such that the ions see a reversal in the field before reaching the electrode and will oscillate between the two electrodes. This critical frequency is given by (for a uniform electric field)[6]

$$f_c = \frac{\mu_+ E_0}{\pi d}, \tag{1}$$

where μ_+ is the ion mobility, E_0 is the peak electric field, and d is the separation between the electrodes. Our previous studies in a coaxial geometry showed a significant lowering (less than 50%) of the field required to initiate a discharge compared to the uniform breakdown static fields.[9] For frequencies about two orders of magnitude higher (microwave) than f_c, the electrons start to get trapped and the diffusion controlled breakdown mechanism takes over. Because of the accumulation of charge, the breakdown at frequencies above f_c requires lower fields than those at static voltages.[8]

In this paper, we present theoretical results and numerical simulations of a novel plasma generation method based on a spatially and temporally varying electric field. The experimental work based on the theory is being carried out and will be published when the results are available. We excite a set of electrodes in such a way that it produces a spatially varying electric field; in particular, tangential components of field lines are introduced.

Rotating electric fields are often used as Penning and RF traps in atomic and plasma physics studies. With the proper choice of the rotating electric field (between the synchrotron and magnetron frequency), stable confinement of space charge can be achieved. Dipole and quadrupole rotating fields give rise to different spatial distributions. Hasegawa used a quadruple rotating field with six azimuthal electrodes and demonstrated that the plasma confinement depends on the rotation frequency and concluded that it performed better than a dipole field for a single species of space charge.[10]

From the above discussion, it is evident that a rotating electric field has the potential to control the spatial distribution of space charge, which will lead to a glow-like diffused discharge. Here, we introduce a unique solution to overcome the fundamental limitation of scaling by temporally confining charged particles and spatially disbursing them by manipulating the electric field. This is done by creating a rotating AC electric field.

The plasma source is a cylindrical geometry with a set of conformal azimuthal electrodes along the length of the outer surface of an insulator, as shown in Fig. 1. This configuration does not require an inner concentric electrode to create an electric field. The excitation of the electrodes at a radius R is of the form

$$V_R(\theta, t) = V_o \cos(\omega t + n\theta), \quad 0 < \theta \le 2\pi, \tag{2}$$

where V_o is the peak voltage of the sinusoid of frequency ω and θ is the anticlockwise angle staring at the positive x-axis and n is the number of cycles. The value of n can be any nonzero integer since

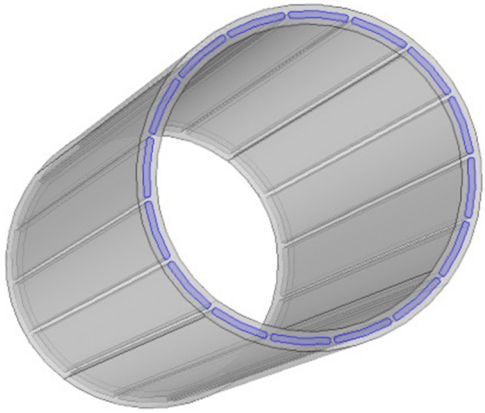

FIG. 1. Electrode geometry.

$n = 0$ would produce a trivial solution of zero electric field in the discharge volume.

The electrostatic potential, $V(r, \theta)$, in the polar coordinate system in the discharge volume is obtained by solving the Laplace equation,

$$\frac{\partial^2 V}{\partial r^2} + \frac{1}{r}\frac{\partial V}{\partial r} + \frac{1}{r^2}\frac{\partial^2 V}{\partial \theta^2} = 0, \tag{3}$$

with Eq. (2) as the boundary condition. Analytical solutions of Eq. (3) on a disk of radius R are given by

$$V(r, \theta) = V_o \left(\frac{r}{R}\right)^n \cos(\omega t + n\theta). \tag{4}$$

The gradient of this electrostatic potential gives the electric field E,

$$E(r, \theta) = n\frac{V_o}{R}\left(\frac{r}{R}\right)^{n-1}\left[(-\cos(\omega t + n\theta)\vec{e_r} + \sin(\omega t + n\theta)\vec{e_\theta}\right]. \tag{5}$$

The spatial distribution of the electric field depends very strongly on n. The magnitude is independent of the azimuthal angle, θ, but the radial and tangential components are strong functions of θ. For $n = 1$ (dipole field), the magnitude of the field is constant throughout the volume of the cylinder, and as "n" increases, the electric field shifts toward the outer surface. The magnitude of the field is linear in the radial direction for $n = 2$ (quadrupole), and the increasing value of "n" produces n-times the uniform dipole field at the boundary. This suggests a unique method of initiating a discharge with high n and subsequently reducing n to the uniform dipole field to obtain a uniform discharge.

The simulation of a charged particle trajectory without space charge was done to understand the confinement of ions in the discharge volume. The position as a function of time is obtained by solving the following equation for a positive nitrogen ion at a pressure of 10 Torr,

$$\frac{d\vec{r}}{dt} = \frac{\partial r}{\partial t}\vec{e_r} + r\frac{\partial \theta}{\partial t}\vec{e_\theta} = \mu_+ \mathbf{E}(\mathbf{r}, \boldsymbol{\theta}, \mathbf{t}). \tag{6}$$

As expected, the simulations show that the confinement is dependent on the voltage peak magnitude and electrode phase (n), discharge tube diameter, the ion mobility (μ_+), and the applied frequency. However, the trajectory of an ion at an arbitrary position in

the rotating electric field was determined to be very sensitive to the initial position due to the nonlinear nature of the solution to Eq. (6). In particular, ion confinement near the center of discharge can be achieved for frequencies lower than f_c obtained from Eq. (1). This could have implications in the reduction of breakdown voltages at frequencies lower than f_c.

Next, we studied the motion of particles when space charge starts to distort the external applied field. The consistent set of equations containing the basic physics necessary for modeling space charge dominated transport are the continuity equations for electrons and positive ions coupled with Poisson's equation for the electric field, along with various constitutive relations for the drift velocities and ionization coefficient is given by[11]

$$\frac{\partial n_e}{\partial t} + \vec{\nabla}\cdot\left(\vec{v_e} n_e\right) - D_e\nabla^2 n_e = \alpha n_e\left|\vec{v_e}\right| + S, \tag{7}$$

$$\frac{\partial n_+}{\partial t} + \vec{\nabla}\cdot\left(\vec{v_+} n_+\right) - D_+\nabla^2 n_+ = \alpha n_e\left|\vec{v_e}\right| + S, \tag{8}$$

$$\nabla^2\Phi = -\frac{\rho}{\epsilon_0} = \frac{-q(n_+ - n_e)}{\epsilon_0}, \tag{9}$$

where n_e, $\vec{v_e}$, D_e, n_+, $\vec{v_+}$, and D_+ are the particle density, drift velocity, and diffusivity for electrons and positive ions, respectively, α is the Townsend ionization coefficient, Φ is the electrostatic potential, q is the unsigned electron charge, and ε_0 is the permittivity of free space. In electronegative gases, negative ion formation by electron attachment will have a significant impact on the transport of space charge and should be included in the continuity equations.[12] In nitrogen and noble gases, negative ion formation is not important.

The term S in Eqs. (7) and (8) represents additional generation mechanisms such as photoionization. Ionization fronts such as streamers require an additional electron source in front for propagation. The usual mechanism is photoionization. However, remnant plasma from previous discharges can also have a similar effect as photoionization. In this work, the photoionization effect is simulated by adding a low background plasma density of 10^5 cm^{-3} which has no effect on the applied electric field. Studies of the detailed effect of such background charges have been presented in Ref. 11.

In the region of operation, for pressure P, in Torr, and electric field E, in V/cm, we used[11]

$$\alpha = 5.7Pe^{-260P/E}\ \text{cm}^{-1}$$

and the electric field dependence of the electron and ion drift velocities is well approximated by a simple constant mobility model,[11]

$$\mu_e = 2.9\times\frac{10^5}{P}\ \frac{\text{cm}^2}{\text{V s}},$$

$$\mu_p = 2.6\times\frac{10^3}{P}\ \frac{\text{cm}^2}{\text{V s}}.$$

For numerical calculations, we used a cylindrical geometry with no variation in the z-direction. We are interested in observing the charge motion in the r-θ plane. We simulated the time evolution of electrons and positive ions self-consistently by solving the Poisson equation for the electric field due to space charge after every time step. We ignored diffusion, and the convective contribution to the density derivative is

$$\left.\frac{\partial N}{\partial t}\right|_{convective} = -\vec{\nabla}\cdot(N\vec{v}) = \frac{-\nabla f}{\nabla vol}, \tag{10}$$

where N is the density of the relevant species, $\vec{v}$ is the drift velocity, and ∇f is the net particle flux leaving a volume, $\nabla\vec{v}ol$. We used a donor cell algorithm with Eulerian time integration to numerically determine the particle densities.

The Poison equation is solved in two dimensions with the axial dimension being infinite. This is a simplification which tends to smooth the spatial electric fields. The Poisson's equation for this two-dimensional problem is solved using Green's theorem. Due to the cylindrical symmetry, a Green's function can be readily constructed and lends itself to quick explicit calculation of the potential due to space charge. The potential inside a grounded cylinder of radius, R, for a wire having a unit charge per unit length gives Green's function,

$$G(r,\theta,r',\theta') = \frac{1}{4\pi\varepsilon_0}\left[-\ln\left(r^2 - 2r'r\cos(\theta-\theta') + r'^2\right) + \ln\left(r^2 - 2\frac{R^2}{r'}r\cos(\theta-\theta') + \left(\frac{R^2}{r'}\right)^2\right) + 2\ln\left(\frac{r'}{R}\right)\right]. \tag{11}$$

The potential due to a two-dimensional charge distribution $\rho(r', \theta')$ can be obtained from the following integral:

$$V(r,\theta) = \int_0^R\int_0^{2\pi} G(r,\theta,r',\theta')\rho(r',\theta')r'dr'd\theta'. \tag{12}$$

A set of simulations was carried out for N_2 at a pressure of 10 Torr for a V_0 = 500 V and a radius R = 10 mm. This produces a reduced electric field which is about 7.5% higher than the static electric field required for the breakdown of a parallel plate gap.[11] The simulations were done at a relatively low pressure because the charge growth is slower and the species can be followed for a longer duration over a larger spatial region without numerical instabilities. For these simulations, we assumed that the Townsend phase (space charge free) of the discharge is completed and the avalanche growth produces regions of space charge. In particular, we assumed initial charge densities (for both electron and positive ion) of a two-dimensional Gaussian distribution with 1/e radii of R/10 and π/10 in the r and θ direction, respectively. The peak value of the Gaussian distribution was chosen to be 5×10^{14} m^{-3} which did not appreciably distort the applied field. We inserted two peaks at two different positions to demonstrate the positional dependence of the space charge transport. The first peak was placed at an angular position with zero tangential component of the applied electric field, and the second peak was at a position where the radial component is zero, and these correspond to θ = 0 and θ = π/2 in Eq. (5), respectively.

The simulations presented in this work are to demonstrate the charge transport in the bulk. However, surfaces will play an important role depending on the frequency of the applied voltage. The discharge of interest in this work is similar to the dielectric barrier discharge: The charges will accumulate on the surfaces and will be replaced by charges of opposite polarity when the voltage reverses. The surface charges impact the electric field, but the effect is

low for high frequencies (above 50 kHz) due to field reversal, as described in Eq. (1).

As the simulation proceeds in time, the space charge builds up due to electron impact ionization. Eventually, the field becomes localized and the numerical model is no longer valid. The electron density contour plots for three different times are shown in Fig. 2. The simulation time is much smaller compared to the time period of the applied field; therefore, the applied field can be considered static for the duration of the simulation. The path of the electrons is determined by the applied field, and clearly, the starting position of the space charge determines its progress in time.

In conventional coaxial geometries, the field lines are radial and maximum at the surface of the concentric inner electrode. The multi-phase excitation under consideration produces a different spatial field distribution, resulting in space charge that is distributed throughout the volume of the discharge. Initially, the charge densities are low and the movement of electrons is not influenced by positive ions. However, as the densities increase due to impact ionization, the ion density tends to follow the shape and size of the electron density. This is similar to a streamer, where the bulk is close to neutral with low field penetration.[11,12]

The positive ion density at 1.6 ns is shown in Fig. 3. Since the mobility of the positive ion is two orders of magnitude smaller than that of electrons, the ions can be considered static for the time scales shown. The positive ion buildup away from the initial peaks is due to electron impact ionization.

The space charge (difference between the ion and electron densities) is mostly localized at the ionization front changing sign over small spatial dimensions, which causes a peaking effect of the electric field at the front. The magnitude of the electric field is shown in Fig. 4. For the dipole mode, the magnitude of the applied electric field is constant at 500 V/cm and at 1.6 ns, the peak field is about 850 V/cm due to space charge.

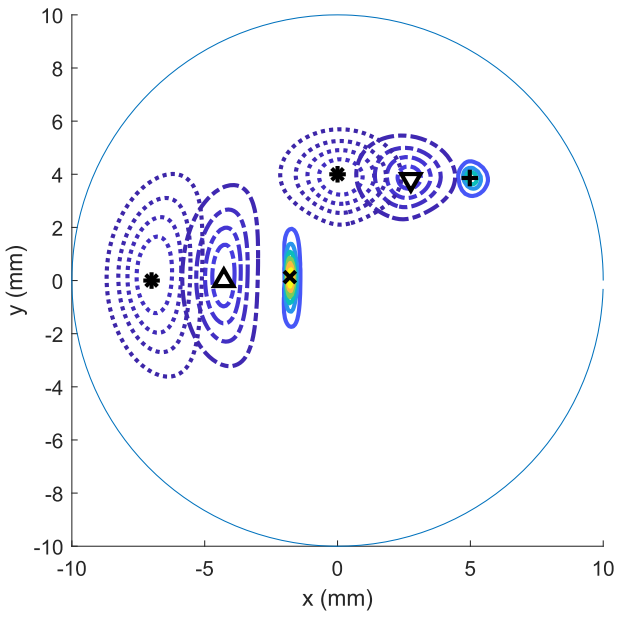

FIG. 2. Contour plots of the electron density at three different times: * is at 0 ns with a peak value of 5×10^{14} m^{-3} and contour intervals of 10^{14} m^{-3}; Δ and ∇ are at 0.8 ns with peaks of 1.06×10^{15} m^{-3} and 0.96×10^{15} m^{-3}, respectively, and contour intervals of 2×10^{14} m^{-3}; and $\times$ and + are at 1.6 ns with peaks of 10^{16} m^{-3} and 6×10^{15} m^{-3}, respectively, with contour intervals of 1.5×10^{15} m^{-3}.

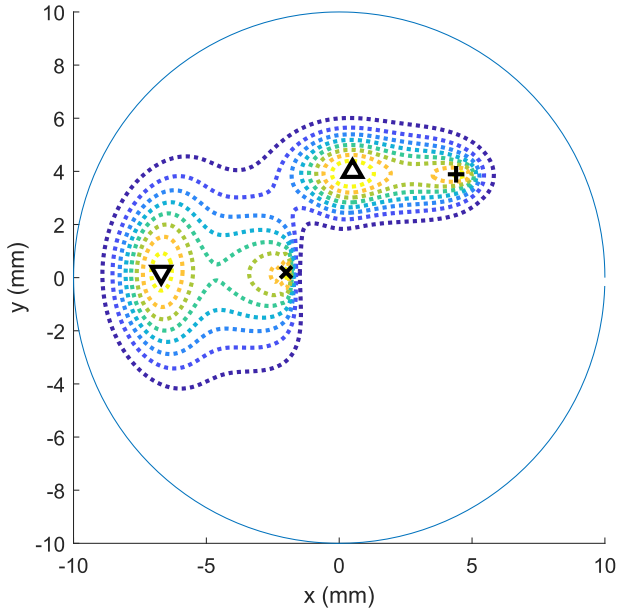

FIG. 3. Positive ion density contours at 1.6 ns. Δ, ∇, +, and $\times$ are peak values of 5×10^{14} m^{-3}. Contour intervals are 6.8×10^{14} m^{-3}, 6.4×10^{14} m^{-3}, 6.3×10^{14} m^{-3}, and 6.4×10^{14} m^{-3}, respectively.

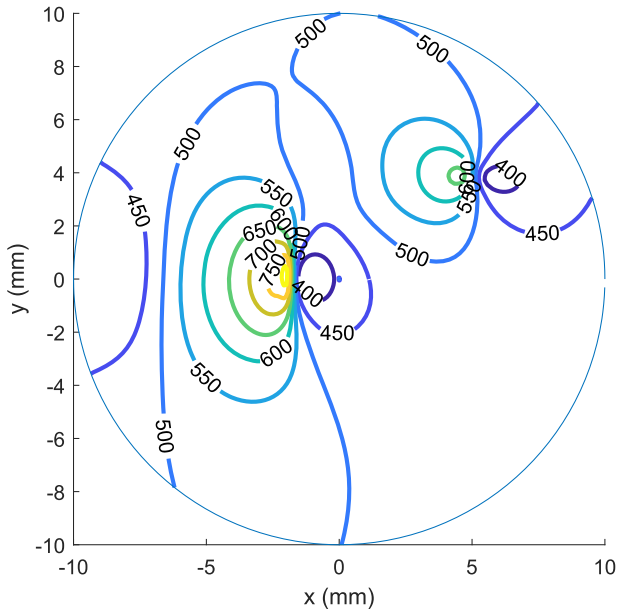

FIG. 4. Contour plot of the magnitude of the electric field. Contour intervals at 50 V/cm.

The simulation results suggest that with the proper choice of operating parameters, the space charge can be distributed throughout the volume of the discharge. The discharge is expected to behave like a continuous RF discharge but operating at lower frequencies (100 kHz). Typical sub-atmospheric pressure discharges are limited to electron densities below $10^{11}/cm^3$.[13] At the other extreme of non-thermal plasma are the micro-discharges in dielectric barrier discharge, which reach densities of 10^{14}–10^{15} cm^{-3}.[14] The current atmospheric pressure diffused RF discharges, although small in volume, produce electron densities in the range of 10^{12} cm^{-3}.[14] Due to space charge dispersion resulting in the prevention of micro-arcs, the proposed method has the potential to produce large-volume plasma with densities approaching 10^{13} cm^{-3} for large scale plasma chemistry applications and light sources.

We have investigated the effect of space charge distribution on an electrical discharge due to a temporally and spatially varying electric field. This study will lead to the creation of a scalable (volume and pressure) non-thermal plasma by controlling the space charge distribution to achieve a controllable large-volume/surface dense plasma under ambient conditions. Some of the salient advantages over the existing methods are as follows: no inner electrode is needed for the cylindrical discharge geometry, the discharge can produce dense uniform plasma over larger volumes, and a higher power input can be achieved as the power per string requirement would be significantly reduced.

The hardware implementation of the proposed device is being carried out in our laboratory. The proof of concept will be done with eight phase-staggered sinusoidal voltages in the frequency range of 50–100 kHz. The phase-staggered voltages will be generated digitally with field programmable gate arrays (FPGAs) followed by digital to analog conversion. These waveforms will be amplified to the required high voltage with power operational amplifiers and MOSFETs. Due to the distributed nature of the excitation, the power requirements are modest for each string. Electrical and optical diagnostics will be used to characterize the discharge.

This material is based on the work supported by the U.S. Department of Energy, Office of Science, Office of Fusion Energy Sciences, under Award No. DE-SC0020183.

REFERENCES

[1] K. H. Becker, U. Kogelschatz, K. H. Schoenbach, and R. J. Barker, *Non-Equilibrium Air Plasmas at Atmospheric Pressure* (Institute of Physics Publishing, Bristol, 2005).
[2] U. Kogelschatz, "Dielectric-barrier discharges: Their history, discharge physics, and industrial application," Plasma Chem. Plasma Process. **23**, 1 (2003).
[3] R. Dorai and M. J. Kushner, "A model for plasma modification of polypropylene using atmospheric pressure discharges," J. Phys. D: Appl. Phys. **36**, 666 (2003).
[4] E. E. Kunhardt, "Generation of large-volume, atmospheric-pressure, nonequilibrium plasmas," IEEE Trans. Plasma Sci. **28**, 189 (2000).
[5] A. Fridman, A. Chirokov, and A. Gutsol, "Non-thermal atmospheric pressure discharges," J. Phys. D: Appl. Phys. **38**, R1 (2005).
[6] Y. P. Raizer, *Gas Discharge Physics* (Springer-Verlag, 1987), p. 239.
[7] E. Nasser, *Fundamentals of Gaseous Ionization and Plasma Electronics* (Wiley-Interscience, NY, 1971), p. 363.
[8] A. Schutze, J. Y. Jeong, S. E. Babayan, J. Park, G. S. Selwyn, and R. F. Hicks, "The atmospheric-pressure plasma jet: A review and comparison to other plasma sources," IEEE Trans. Plasma Sci. **26**, 1685 (1998).
[9] S. Shakir, S. Mynampati, B. Pashaie, and S. K. Dhali, "rf-generated ambient-afterglow plasma," J. Appl. Phys. **99**, 073303 (2006).
[10] T. Hasegawa, M. J. Jensen, and J. J. Bollinger, "Stability of a Penning trap with a quadrupole rotating electric field," Phys. Rev. A **71**, 023406 (2005).
[11] S. K. Dhali and P. F. Williams, "Two-dimensional studies of streamers in gases," J. Appl. Phys. **62**(12), 4696 (1987).
[12] S. K. Dhali and P. K. Pal, "Numerical simulation of streamers in SF_6," J. Appl. Phys. **63**, 1355 (1988).
[13] L. J. Overzet and M. B. Hopkins, "Comparison of electron-density measurements made using a Langmuir probe and microwave interferometer in the Gaseous Electronics Conference reference reactor," J. Appl. Phys. **74**, 4323 (1993).
[14] M. Moravej, X. Yang, G. R. Nowling, J. P. Chang, R. F. Hicks, and S. E. Babayan, "Physics of high-pressure helium and argon radio-frequency plasmas," J. Appl. Phys. **96**, 7011 (2004).